International Journal of Scientific Research in Computer Science, Engineering and Information Technology
© 2018 IJSRCSEIT | Volume 3 | Issue 3 | ISSN : 2456-3307

# Analysis of Image Quality using LANDSAT 7 ETM+ and Gaussian Filter

**A. L. Choodarathnakara*[1] and Sinchana G S[2]**

*[1]Assistant Professor, Dept. of Electronics & Communication Engineering, Government Engineering College, Kushalnagar, Karnataka, India

[2]UG Scholar, USN: 4GL15EC045, Department of E&C Engineering, GEC, Kushalnagar, Karnataka, India

## ABSTRACT

Interpretation of image contents is a significant objective in computer vision and image processing. An image contains different information of scene, such as objects shape, size, color and orientation, but discrimination of the objects from their background is the first essential task that should be performed before any interpretation. Filters re-evaluate the value of every pixel in an image. For a particular pixel, the new value is based on pixel values in a local neighborhood, a window centered on that pixel, in order to reduce noise by smoothing and enhance edges. At the same time as reducing the noise in a signal, it is important to preserve the edges. Edges are of critical importance to the visual appearance of images. So, it is desirable to preserve important features, such as edges, corners and other sharp structures, during the denoising process. In this paper an attempt is made to assess the impact of bandwidth on image quality using Gaussian filter and LANDSAT 7 ETM+ satellite imagery. The study area considered for the experimentation is the Mysore city in the state of Katnataka. From the experimental observations, for a satellite image with high resolution around 30m, the window 5x5 is recommended which improves image while preserving the edges.

**Keywords :** Remote Sensing, Image Processing, Gaussian Filter, LANDSAT 7 ETM+, Matlab.

## I. INTRODUCTION

The filtering methods are used for image enhancement and denoising. There many types of filters are used to enhance an Image. Median filter it would be removing noise in image, but the median filter it depends on mask size chosen. The mask size is larger, then the image become blurring and over smoothing. Image denoising is also called image restoration techniques.

Gaussian filters are the most widely used filters in image processing and extremely useful as detectors for edge detection. It is proven that they play a significant role in biological vision particularly in human vision system. Gaussian based edge detectors are developed based on some physiological observations and important properties of the Gaussian function that enable to perform edge analysis in the scale space. Marr and Hildreth were the pioneers that proposed an edge detector based on Gaussian filter. Their method had been a very popular one, before Sobel released his detector. They originally pointed out the fact that the variation of image intensity (i.e. edge) occurs at different levels. This implied the demand to smoothing filters with different scales, since a single filter cannot be optimal for all possible levels. They suggested the 2D Gaussian function, defined as following, as the smoothing operator.

$$G_\sigma(x,y) = \frac{1}{2\pi\sigma^2}\exp\left(-\frac{x^2+y^2}{2\sigma^2}\right) \quad \ldots\ldots \quad (1)$$

Where, $\sigma$ is the standard deviation, and (x, y) are the Cartesian coordinates of the image pixels. They showed that by applying Gaussian filters of different scales i.e., $\sigma$ to an image; a set of images with different levels of smoothing will be obtained.

There are advantages for the Gaussian filters that make it unique and so important in edge detection. The first concerns to its output. It is proven that when an image is smoothed by Gaussian filter, the existing zero-crossings (i.e. detected edges) disappear as moving from fine-to-coarse scale, but new ones are never created.

This unique property makes it possible to track zero-crossings (i.e. edges) over a range of scales, and also gives the ability to recover them at sufficiently small scales. Yuille and Poggio proved that with the Laplacian, the Gaussian function is the only filter in a wide category that does not create zero-crossings as the scale increases. The dual tree complex wavelet transform having the high computational complexity is high compared with wavelet. There are iterative algorithms also used for image denoising. There are landweber, total variation and blinded-convolution methods are resulting good output, but produces moderated quality measure.

In this paper an attempt is made to assess the impact of bandwidth on image quality using Gaussian filter and LANDSAT 7 ETM+ satellite imagery. The study area considered for the experimentation is the Mysore city in the state of Katnataka. From the experimental observations, for a satellite image with high resolution around 30m, the window 5x5 is recommended which improves image while preserving the edges.

## II. DIGITAL IMAGE PROCESSING

Digital Image is a representation of an object, which comprised of discrete picture elements (Pixel), each having a digital number generated by the electro-optical scanners of the satellite like Landsat MSS, IRS etc. In digital image, the data is arranged in a matrix of a number or brightness value and is located in X, Y-coordinate system. A pixel is "a two dimensional picture element that is the smallest non-divisible element of a digital image". The dataset may be of multispectral bands and each pixel has brightness value or digital number from each of these multispectral bands. The digital numbers representing the variation in the intensity of radiant energy emitted from different earth surface features. The digital number starts from 0 and goes up to a higher value on the gray scale, for example, 0 to 127 in IRS series. Lower the brightness value in the gray scale, lower the intensity of radiant energy from that area of the ground, higher the value, higher the intensity of the radiant energy of the area of the ground. In 7-bit data, 0 represents black and 127 represents white.

The first step towards designing an image analysis system is digital image acquisition using sensors in optical or thermal wavelengths. A two dimensional image that is recorded by these sensors is the mapping of the three-dimensional visual world. The captured two dimensional signals are sampled and quantized to yield digital images. Sometimes we receive noisy images that are degraded by some degrading mechanism. One common source of image degradation is the optical lens system in a digital camera that acquires the visual information. If the camera is not appropriately focused then we get blurred images. Here the blurring mechanism is the defocused camera. In some cases there may be a relative motion between the object and the camera. Thus if the camera is given an impulsive displacement during the image capturing interval while the object is static, the resulting image will invariably be blurred and noisy. In some of the above cases, we need appropriate techniques of refining the images so that the resultant images are better visual quality, free from aberrations and noises. Hence, image enhancement, filtering, and restoration have

been some of the important applications of image processing since the early days of the field.

## III. STUDY AREA AND METHODOLOGY

### A. Study Area

The Mysore, officially renamed as Mysuru, is the third most populous city in the state of Karnataka, India located at the base of the Chamundi Hills about 146 km (91 mi) southwest of the state capital Bangalore. It is spread across an area of 128.42 km$^2$ (50 sq mi) & Mysore is located at 12.30°N 74.65°E and has an average altitude of 770 meters (2,526 ft). People in and around Mysore extensively use Kannada as medium of language. Mysore has several lakes, such as the Kukkarahalli, the Karanji, and the Lingambudhi lakes. In 2001, total land area usage in Mysore city was 39.9% residential, 16.1% roads, 13.74% parks and open spaces, 13.48% industrial, 8.96% public property, 3.02% commercial, 2.27% agriculture and 2.02 water. The city is located between two rivers: the Kaveri River that flows through the north of the city and the Kabini River, a tributary of the Kaveri that lies to the south. According to the provisional results of the 2011 national census of India, the population is 887,446.

Urban growth and expansion is managed by the Mysore Urban Development Authority (MUDA), which is headed by a commissioner. Its activities include developing new layouts and roads, town planning and land acquisition. One of the major projects undertaken by MUDA is the creation of an Outer Ring Road to ease traffic congestion. Mysore has a tropical savanna climate designated under the Koppen climate classification. The main seasons are summer from March to June, the monsoon season from July to November and winter from December to February. The highest temperature recorded in Mysore was 39.4 °C (103 °F) on 4 April 1914, and the lowest was 7.7 °C (46 °F) on 16 January 2012. The city's average annual rainfall is 804.2 mm (31.7 in). Drinking water for Mysore is sourced from the Kaveri and Kabini rivers. The city got its first piped water supply when the Belagola project was commissioned in 1896. As of 2011, Mysore gets 42.5 million gallons water per day. Mysore sometimes faces water crises, mainly during the summer months (March–June) and in years of low rainfall. The city has had an underground drainage system since 1904. The entire sewage from the city drains into four valleys: Kesare, Malalavadi, Dalavai and Belavatha. In an exercise carried out by the Urban Development Ministry under the national urban sanitation policy, Mysore was rated the second cleanest city in India in 2010 and the cleanest in Karnataka.

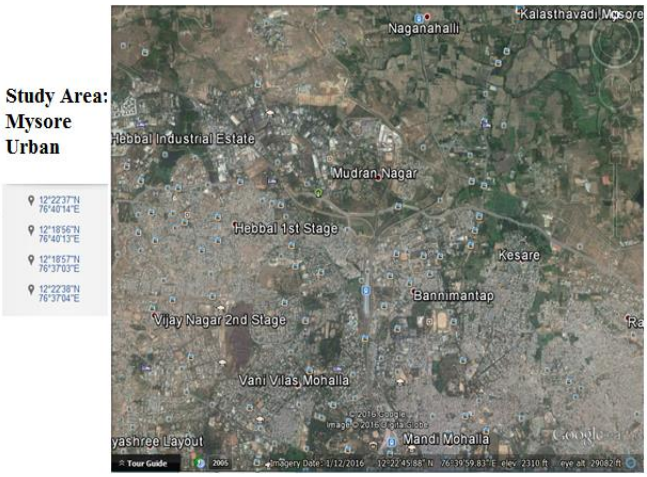


**Figure 1.** Google Earth Snapshot of Mysore Study Area

### B. Data Products

The Table I provide the specification of satellite image data products used in this work. Another data used is the visual band multi spectral data downloaded from www.wikimapia.com. The Table II specifies the characteristics of LANDSAT 7 ETM+ band with ground features.

**Table I Details of Satellite Data Products Used**

| SL. No | Satellite and data type | Data of acquisition | Spectral Resolution | Spatial Resolution |
|---|---|---|---|---|
| 1. | Land Sat ETM 7 | 2010 | Blue(0.45-0.515µm)<br>Green(0.525-0.605µm)<br>Red(0.632-0.69µm)<br>Near Infrared(0.75-0.90µm)<br>Short wave IR-1(1.55-1.75µm)<br>Thermal IR(10.4-12.5µm)<br>Short wave IR -2(2.09-2.35µm) | 30.0m |
| 2. | Google Earth | April 2016 | - | - |

**Table II LANDSAT 7 ETM+ Bands used with Ground Features**

| Ground feature | Band used |
|---|---|
| Water | 1,2,3; 1,2,4; 1,4,5 |
| Urban | 1,2,3; 1,4,5 |
| Farmland | 1,2,3; 1,4,5 |
| Forest | 1,2,3; 1,4,5 |
| Salt scald | 1,2,3 |
| Scrub | 1,4,5 |
| Vegetation | 1,4,7 |

## C. Methodology

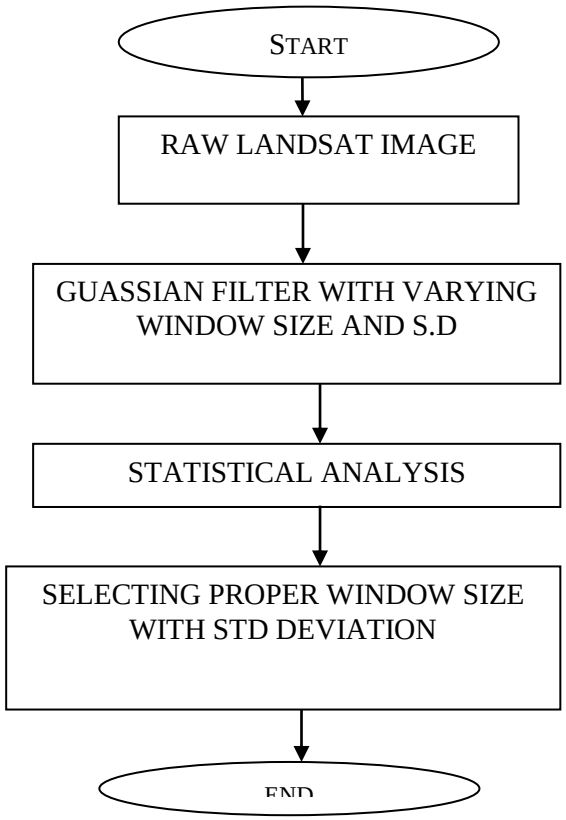


**Figure 2**. Flowchart of the Experimental Setup

1) Flowchart of the Proposed Methodology: The Figure 2 shows the flowchart of the experimental setup.

2) Gaussian Filtering: In this work, Gaussian filter is used to illustrate how frequency domain filters can be used as guides for specifying the coefficients of some of the small masks. Filters based on Gaussian forward and Inverse Fourier Transform of a Gaussian function is the real Gaussian functions.

Let, H(u) denote the 1-D frequency domain Gaussian filter.

$$H(u)=Ae^{-u^2/2\sigma^2} \quad \ldots\ldots \quad (2)$$

Where, $\sigma$ is the standard deviation of the Gaussian curve. The corresponding filter in the spatial domain obtained by taking the inverse Fourier transform of H(u).

$$h(x)=\sqrt{2\pi\sigma}Ae^{-2\pi^2\sigma^2x^2} \quad \ldots\ldots\ldots \quad (3)$$

1.1) Gaussian Low-pass Filters: The 2-D of Gaussian low pass filter is given by,

$$H(u,v)=e^{-D^2(u,v)/2\sigma^2} \quad \ldots\ldots \quad (4)$$

Where, D(u,v) is the distance from center of the frequency rectangle. As before, $\sigma$ is measure of spread about the center. By letting $\sigma = D_0$, we can express the filter using the notation of the other filters

$$H(u,v)=e^{-D^2(u,v)/2D_0^2} \quad \ldots\ldots \quad (5)$$

Where, $D_0$ is the cutoff frequency, when D (u, v) = $D_0$, the GLPF is down to 0.607 of its maximum value.

1.2) Gaussian High-pass Filters: The transfer function of the GHPF with cut-off frequency locus at a distance $D_0$ from center of the frequency rectangle is given by,

$$H(u,v)=1-e^{-D^2(u,v)/2D_0^2} \quad \ldots\ldots \quad (6)$$

## IV. RESULTS AND DISCUSSION

### A. Matlab Window for Gaussian Filter

The Figure 3 shows the main interface for the MATLAB and Figure 4 shows the code of Gaussian filter written in MATLAB language and its execution in Command Window.

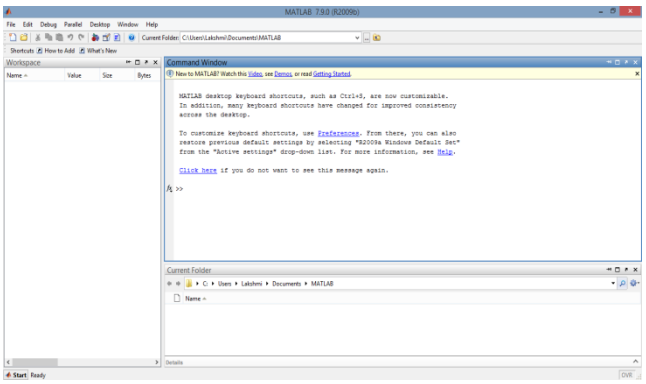

**Figure 3.** The main interface for the MATLAB.

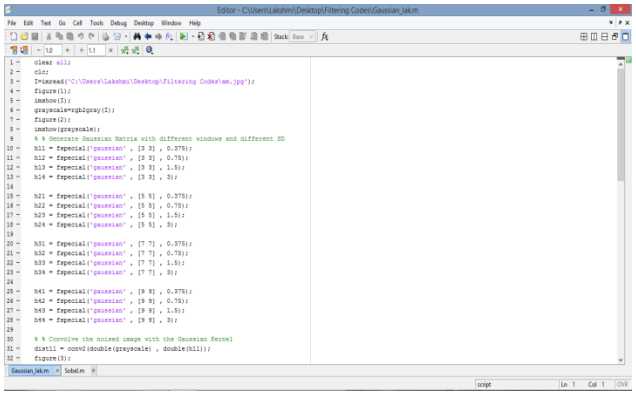

**Figure 4.** The code of Gaussian filter written in MATLAB language.

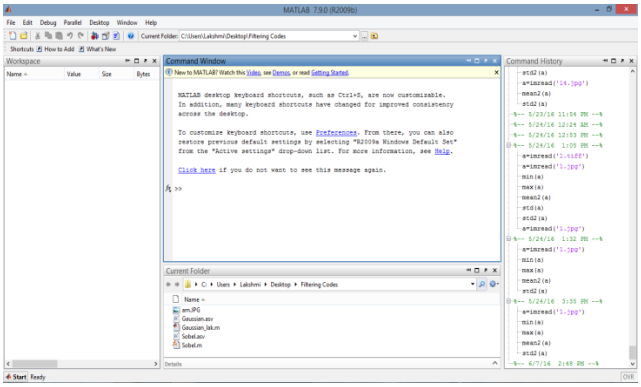

**Figure 5.** Command window to run Gaussian filtering code

The Figure 6 shows the input data from LANDSAT 7 ETM+ satellite image with 28.5m spatial resolution. The Figure 7 shows conversion to gray scale.

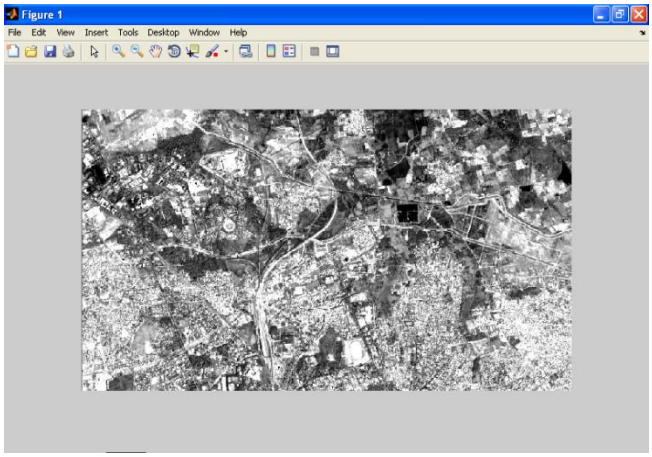

**Figure 6.** Input data from Landsat (28.5 m)

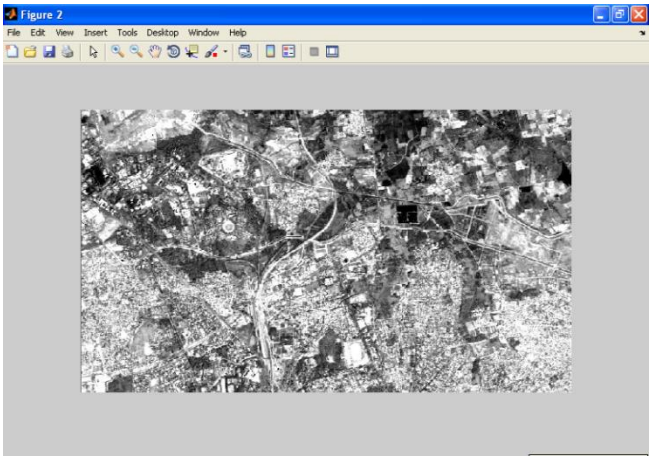

**Figure 7.** Conversion to gray scale

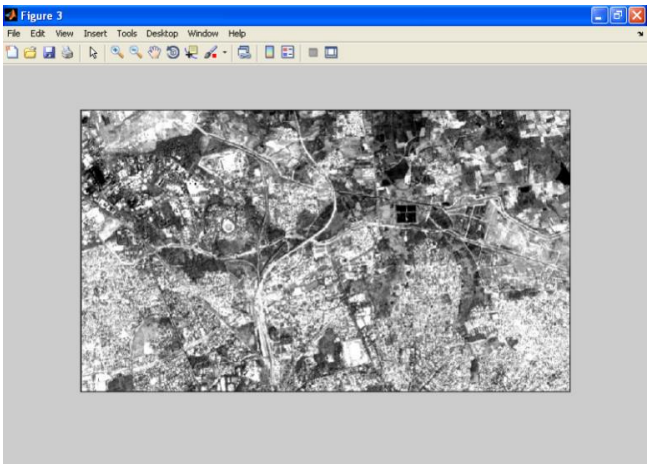

**Figure 8.** Window 3X3 with Standard Deviation 0.375

The Figures 8, 9, 10 & 11 shows the images obtained for 3x3 bandwidth with different Standard Deviation 0.375, 0.75, 1.5 & 3 respectively.

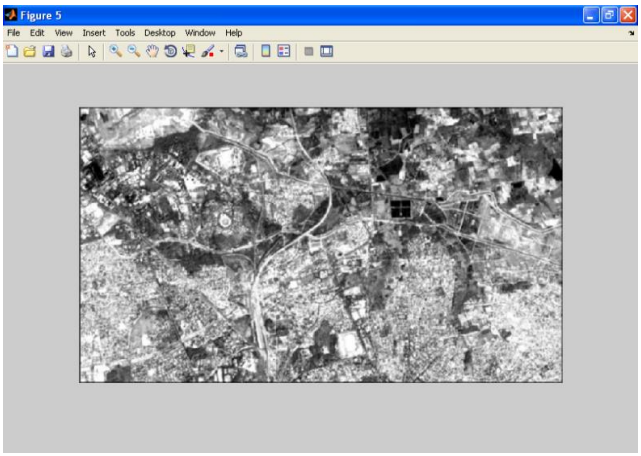


**Figure 9.** Window 3X3 with Standard Deviation 0.75

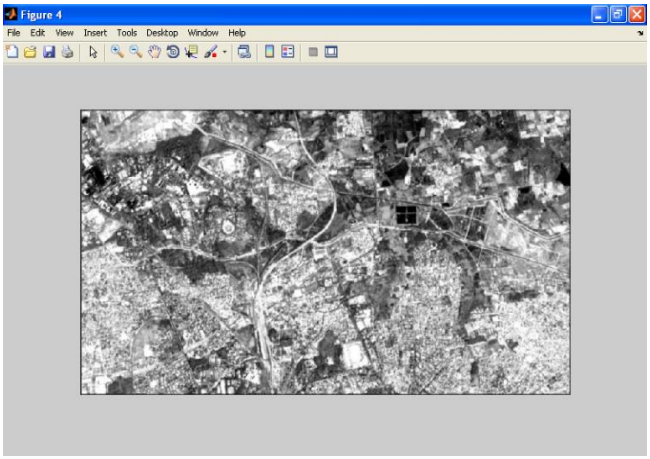


**Figure 10.**Window 3X3 with Standard Deviation 1.5

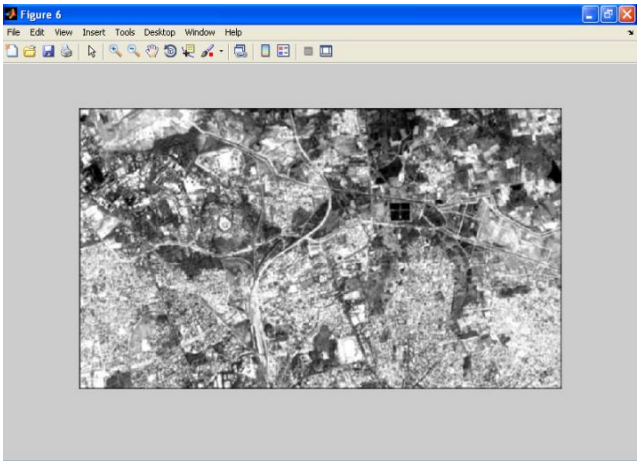


**Figure 11.** Window 3X3 with Standard Deviation 3

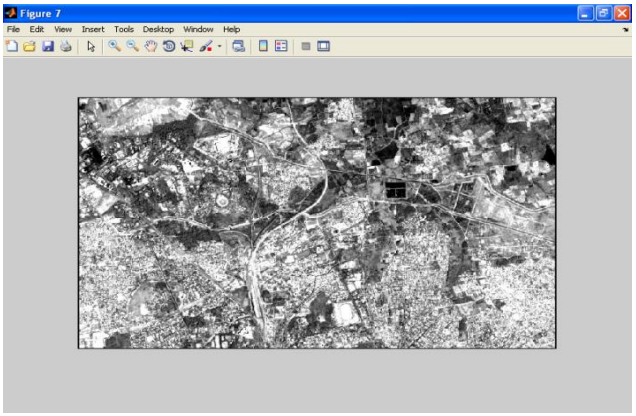


**Figure 12.** Window 5X5 with Standard Deviation 0.375

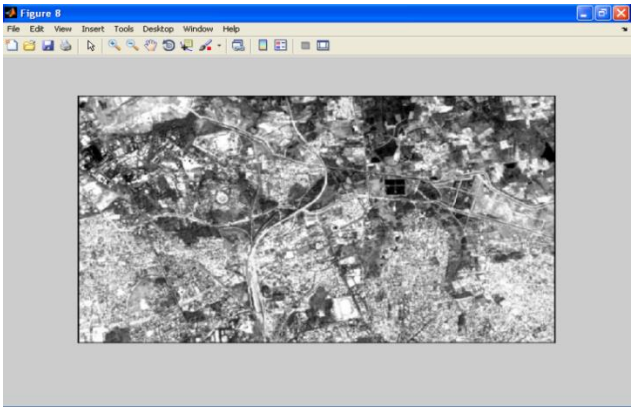


**Figure 13.** Window 5X5 with Standard Deviation 0.75

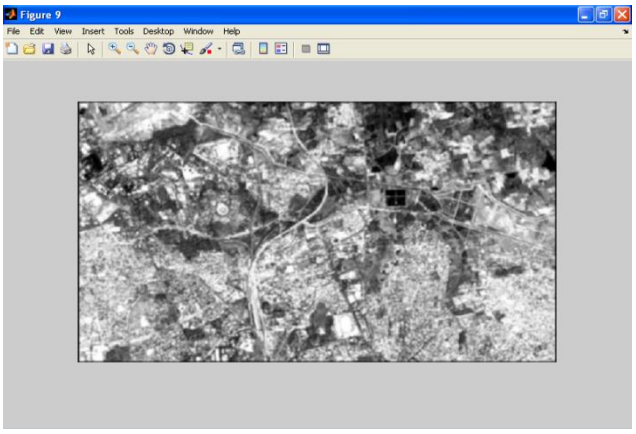


**Figure 14.** Window 5X5 with Standard Deviation 1.5

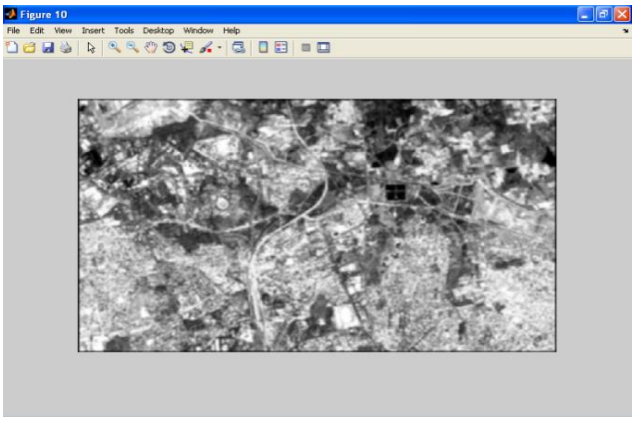


**Figure 15.** Window 5X5 with Standard Deviation 3

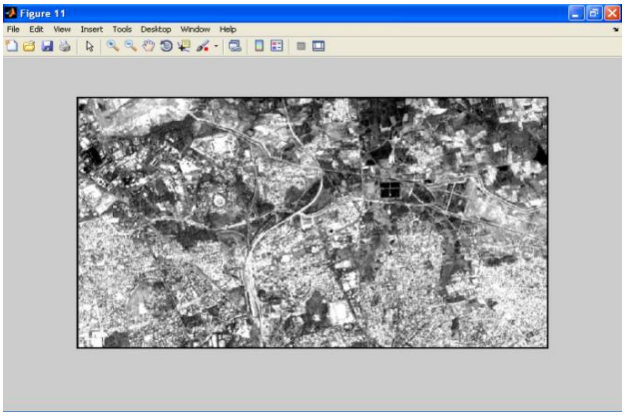


**Figure 16.** Window 7X7 with Standard Deviation 0.375

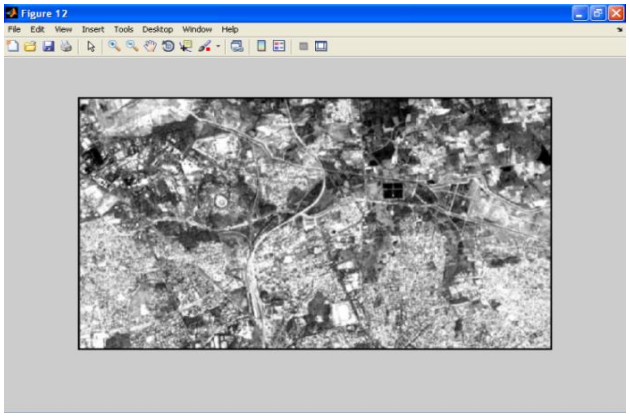


**Figure 17.**Window 7X7 with Standard Deviation 0.75

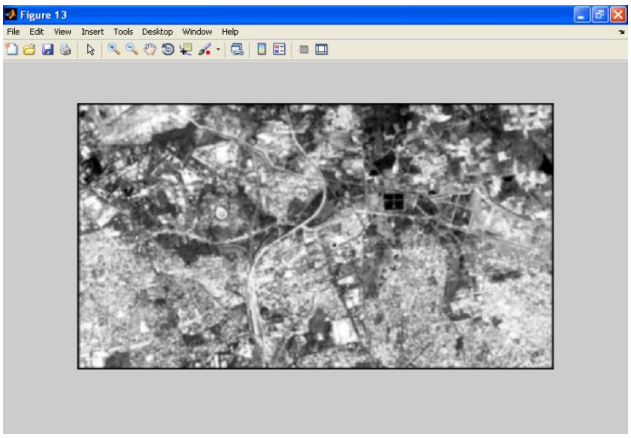


**Figure 18.** Window 7X7 with Standard Deviation 1.5

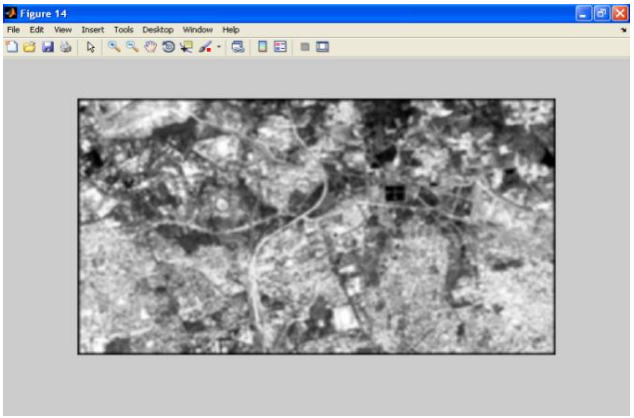


**Figure 19.** Window 7X7 with Standard Deviation 3

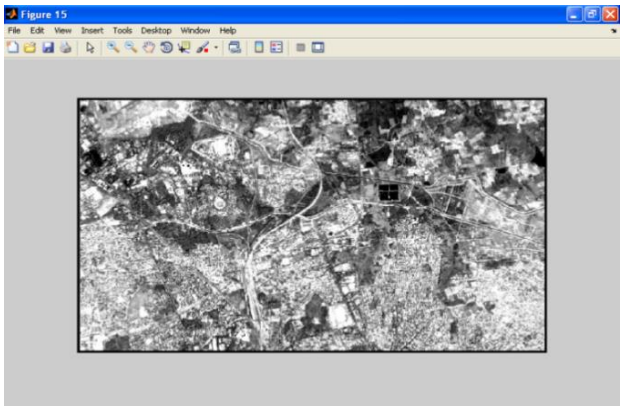


**Figure 20.** Window 9X9 with Standard Deviation 0.375

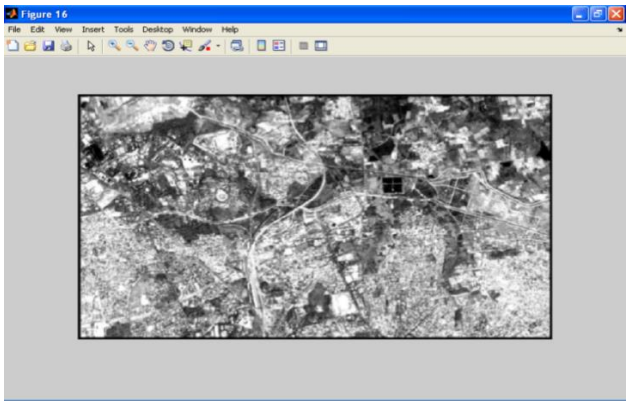

**Figure 21.** Window 9X9 with Standard Deviation 0.75

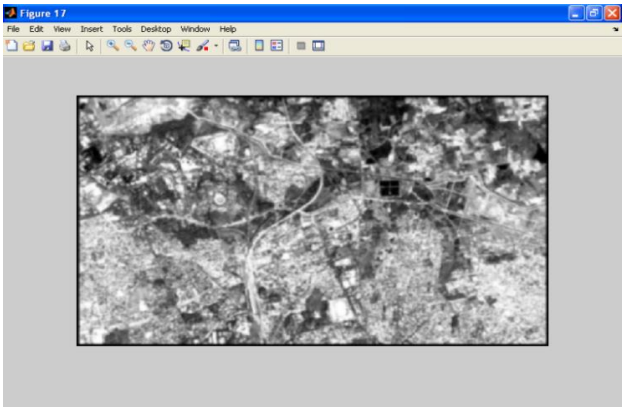

**Figure 22.** Window 9X9 with Standard Deviation 1.5

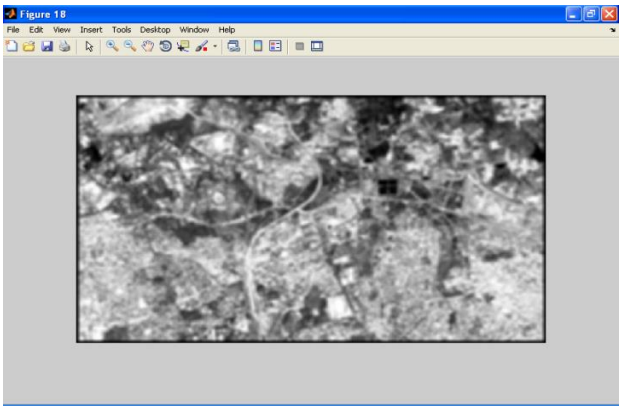

**Figure23.** Window 9X9 with Standard Deviation 3

The Figures 12, 13, 14 & 15 shows the images obtained for 5x5 bandwidth with different Standard Deviation 0.375, 0.75, 1.5 & 3 respectively.

The Figures 16, 17, 18 & 19 shows the images obtained for 7x7 bandwidth with different Standard Deviation 0.375, 0.75, 1.5 & 3 respectively.

The Figures 20, 21, 22 & 23 shows the images obtained for 9x9 bandwidth with different Standard Deviation 0.375, 0.75, 1.5 & 3 respectively.

**Table 3.** Gaussian Filter Statistical Results for different window sizes

| Filter Window SD | Filter Window Size | Min | Max | Mean | Standard Deviation | SNR |
|---|---|---|---|---|---|---|
| **Original Image** | | **0** | **255** | **146.928** | **67.333** | **2.182** |
| Grayscale | | 0 | 255 | 146.928 | 67.333 | 2.182 |
| 3 | 3 x 3 | 0 | 255 | 146.819 | 57.748 | 2.542 |
| **3** | **5 x 5** | **0** | **255** | **145.707** | **52.121** | **2.795** |
| 3 | 7 x 7 | 0 | 255 | 144.704 | 52.486 | 2.757 |
| 3 | 9 x 9 | 0 | 255 | 144.202 | 51.889 | 2.779 |
| 1.5 | 3 x 3 | 0 | 255 | 146.823 | 58.005 | 2.531 |
| **1.5** | **5 x 5** | **0** | **255** | **145.715** | **55.318** | **2.634** |
| 1.5 | 7 x 7 | 0 | 255 | 144.733 | 55.037 | 2.629 |
| 1.5 | 9 x 9 | 0 | 255 | 144.186 | 55.811 | 2.583 |
| **0.75** | **3 x 3** | **0** | **255** | **146.835** | **59.503** | **2.468** |
| 0.75 | 5 x 5 | 0 | 255 | 145.748 | 59.645 | 2.444 |
| 0.75 | 7 x 7 | 0 | 255 | 144.736 | 60.621 | 2.388 |
| 0.75 | 9 x 9 | 0 | 255 | 144.196 | 61.566 | 2.342 |
| **0.375** | **3 x 3** | **0** | **255** | **146.535** | **66.903** | **2.190** |
| 0.375 | 5 x 5 | 0 | 255 | 145.419 | 67.640 | 2.149 |
| 0.375 | 7 x 7 | 0 | 255 | 144.408 | 68.462 | 2.109 |
| 0.375 | 9 x 9 | 0 | 255 | 143.859 | 69.238 | 2.077 |

## V. CONCLUSION & SCOPE FOR FUTURE WORK

### A. Conclusions

**1) Gaussian Filter:** For satellite image with high resolution around 30m window 5X5 is recommended. It gives the best result and the best enhancement of the image with preserving the edges.

**2) Future Work:** These filtering techniques can be implanted further for different satellite data products. These filtering techniques can be implanted further for more than 9x9 window sizes to identify the impact quality bandwidth on satellite image quality.

## VI. ACKNOWLEDGEMENT

Special thanks to Mr. Nasser Mustafa Saleh Abdin for encouragement, guidance and other contributions to this study. All the Landsat 7 ETM+ data used in this work is downloaded from the USGS web (http://glovis.usgs.gov), Special thanks to the group.

The authors would like to thank anonymous reviewers for their valuable comments.

## VII. REFERENCES

[1]. Hyder Ali, Sukanesh and Fellow, "An Edge Preserving Denoising Technique for MR Images using Curvelet Transform", Interdisciplinary Journal, Vol. 91, May 2010, pp.3-8.

[2]. Shujun Fu, Qiuqi Ruan, Wenqia Wang and Yu Li, "Adaptive Anisotropic Diffusion for Ultrasonic Image Denoising and Edge Enhancement", International Journal of Information Technology, Vol. 2, No. 4, 2006, pp. 284-287.

[3]. Shujun Fu, QiuqiRuan, Wenqia Wang and Yu Li, "Feature Preserving Nonlinear Diffusion for Ultrasonic Image Denoising and Edge Enhancement", World Academy of Science, Engineering and Technology, Vol. 2, February 2005, pp. 148-151.

[4]. Tanaphol Thaipanich and Jay Kuo, "An Adaptive Nonloca Means Scheme for Medical Image Denoising", In Proceeding of SPIE Medical Imaging.Vol.7623,San Diego, CA, USA, February 2010.

[5]. Su Cheol Kang and Seung Hong Hong, "A Speckle Reduction Filter using Wavelet-Based Methods for Medical Imaging Application", In Proceedings of 23rd Annual International Conference of the IEEE Engineering in Medicine and Biology Society, Vol.3, pp. 2480-2483.

[6]. C. Chao and A. P. Dhawan, "Edge detection using Hopfield neural network", Proc. SPIE, Vol. 2243, 242 (1994); doi:10.1117/12.169971.

[7]. D. Marr and E. Hildreth, "Theory of edge detection" Proc. Royal Society of London, B, 1980, 207, pp. 187–217.

[8]. A. L. Yuille and T. A. Poggio, "Scaling theorems for zero-crossings", IEEE Trans. Pattern Anal Machine Intell. Vol. PAMI-8, Jan, 1986, pp. 15–25.

[9]. Cui F. Y. Zou L. J. and Song B, "Edge Feature Extraction Based on Digital Image Processing Techniques", International Conference on Automation and Logistics, IEEE, 2008, pp. 2320-2324.

[10]. Nadernejad E. Sharifzadeh S. and Hassanpour H, "Edge Detection Techniques: Evaluations and Comparisons", Applied Mathematical Sciences, Vol. 2, No. 31, 2008, pp.1507- 1520.

[11]. Amit Chaudhary, Tarun Gulati, "Segmenting Digital Images Using Edge Detection", International Journal of Application or Innovation in Engineering & Management (IJAIEM), Volume 2, Issue 5, May 2013.

[12]. Simranjit Singh Walia, Gagandeep Singh, "Color based Edge detection techniques – A Review", International Journal of Engineering and Innovative Technology (IJEIT) Volume 3, Issue 9, March 2014.

[13]. Er. Komal Sharma, Er. Navneet Kaur, "Comparative Analysis of Various Edge Detection Techniques", International Journal of Advanced Research in Computer Science and Software Engineering, Vol. 3, Issue 12, December 2013.

[14]. John R. Jensen and Dave C. Cowen," Remote Sensing of Urban/Suburban Infrastructure and Socio-Economic Attributes", Photogrammetric Engineering &Remote Sensing, 1999, pp. 611-622.